Using Normalized Difference Vegetation Index (NDVI) to Identify Hydrocarbon Seepage in Kifl Oil Field and Adjacent Areas South of Iraq

Walid A. Ahmad[1]   Mousa Abdulateef Ahmed[2]   Ghazi H. Al-Sharia[3]
1. College of remote sensing and geophysics, Al-Karkh University-Iraq
2. Department of Earth Science, College of Science, Baghdad University-Iraq
3. Oil Exploration Company, Ministry of Oil-Iraq

Abstract

The study area lies south of Iraq, it covers 4009 km². The data is used in this research comprise Landsat 8 (OLI) data, and Ancillary data such as geological and topographic maps. The study area include the Kifl Oil Field whereas comprise number of important formations for oil production. There are four oil wells drilled in the Kifl Oil Field. Some of them producer of hydrocarbon and others wells have hydrocarbon evidences.The Normalized Difference Vegetation Index (NDVI) is used to identify prospective hydrocarbon seepage areas within the vegetation cover, the magnitude of green vegetation was quantified to levels and separated from other classes. The classification system for the vegetation in the study area is based on four categories: High vegetation density, Moderate vegetation density, Low vegetation density, and no vegetation. The result of classification reveals that low vegetation density areas, and no vegetation areas could be prospective hydrocarbon seepage areas. Supervised classification apply on the gray scale image of NDVI by chosen training areas of dark tones pixels that have values of absorption close to values of water absorption which are illustrated prospective hydrocarbon seepage areas. Three classes in the study area included hydrocarbon seepage class compared with other three classes collected from another near area, this comparison has been proved that there is identical behave of the spectral signatures for all three classes. According to the conclusions, the NDVI is effective to identify hydrocarbon seepage in the study area particularly in the regions characterized by vegetation cover.
Keywords: Landsat 8 (OLI), Hydrocarbon Seepage, NDVI, Threshold, Anaerobic.

1. Introduction

Remote sensing is a suitable tool for direct and indirect detection of the presence of hydrocarbon seepages (Schumacher, 2001). Landsat and other remote sensor have been used in searching for surface indicators of leaking subsurface oil/gas. Oil and gas macroseepage and microseepage are important in petroleum exploration for many reasons, because it can be indicators of petroleum or natural gas reservoirs in the subsurface, and the quality of petroleum can also be recognized before drilling, also seeps are indicators of some structures like fracture zone, and in some cases seepage represent geo-hazards and sources of pollution and greenhouse gases.

The hydrocarbons that escaped from underground reservoirs cause changes in situ or along vertical migration paths and result in anomalies in sediments and soils. The surface changes can be detected by multispectral and hyperspectral remote sensing.

1.1 Aim of the study

The main aim of this study is:
Detection of hydrocarbon seepage using normalized difference vegetation index (NDVI) in Kifl Oil Field and adjacent areas.

1.2 Location of the study area

The study area lies south of Iraq, it covers 4009 km², and determined by the fallowing coordinates (Figure 1).
Longitude   43° 51' 15"   44° 36' 51" E
Latitude   31° 57' 24"   32° 27' 51" N

1.3 Kifl Oil Field

The Kifl Oil Field locates between Al-Najaf and Karbala governorates. (Figure 2), it includes number of formations, but there are two important formations for production oil:

1.3.1 Hartha Formation

The formation is present in a depocenter extending along the western side of the Mesopotamian Zone and along the eastern side of the Salman Zone .The formation was deposited as shoals and banks with rudest debris (Hippurites), oolitic carbonates, sabkha carbonates and evaporates. The formation is up to 450 m thick near Al-Najaf. The Hartha Formation reservoir is found in 30 structures in S, Central and N Iraq. The net reservoir thickness generally does not exceed 45 m. The porosity of the formation where best developed .The API gravity

of its oil ranges from15 to 30° (averaging about 25°) with a sulphur content varying from 1.45-5.9% (averaging about 4%). (Jassim and Goff, 2006).

1.3.2 Zubair Formation

The formation extends from the Tharthar region in central Iraq southwards towards the Iraqi-Kuwalt border; it is >500 m thick in the area S of Baghdad. The formation consists of sandstone and shale. Limestone beds occur in the formation in SE Iraq. The net sand content of the formation generally increases towards the west, from zero near the Iraq Iran border to over 200 m near Zubair in the south and near Karbala to the north. Between Nasiriya and Amara the net sand thickness is about 100m; carbonates comprise about 15% of the formation near Nasiriya and 35% near Amara. Strong oil shows in the formation are also recorded from wells bordering the Euphrates River; Kifl-1 tested 5,600 bll/d from the Zubair Formation. (Jassim and Goff, 2006).
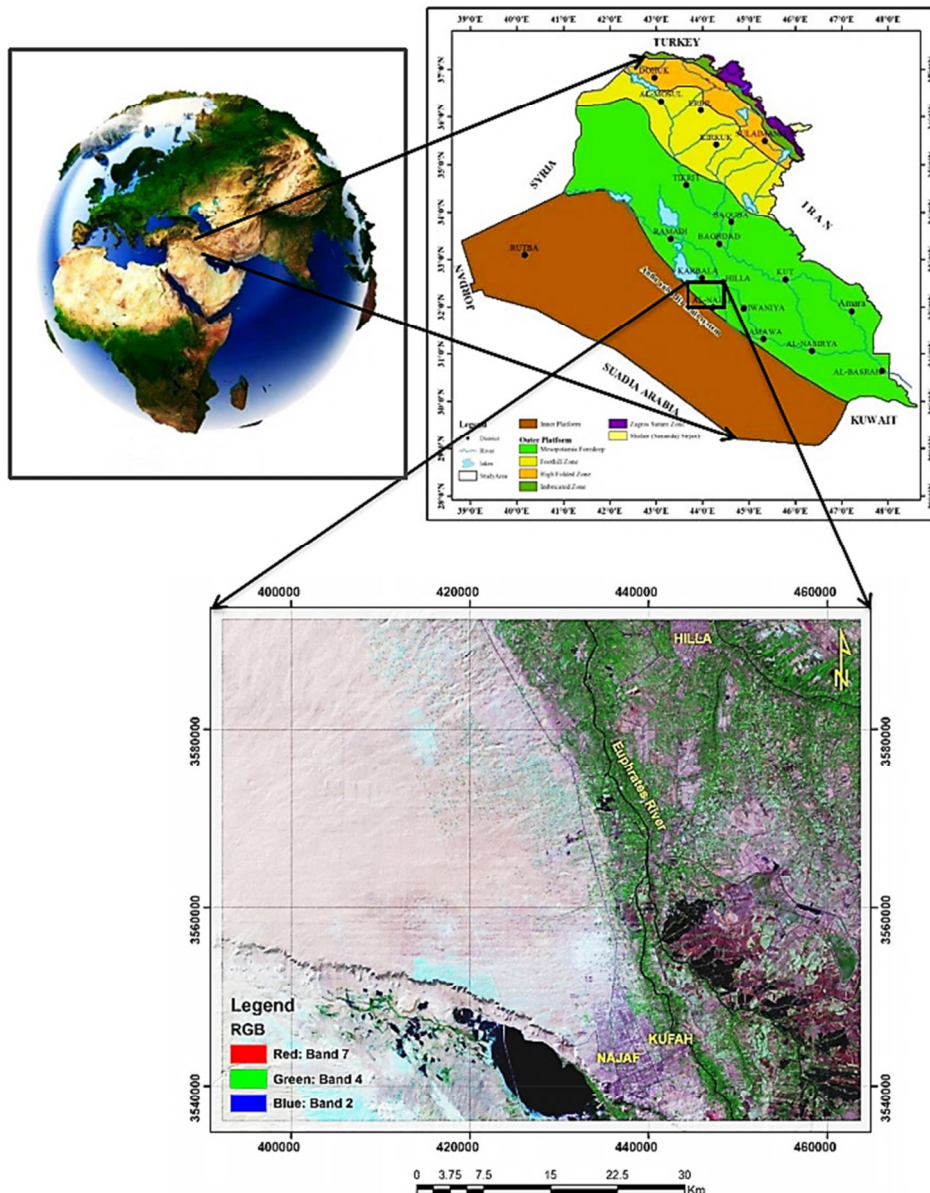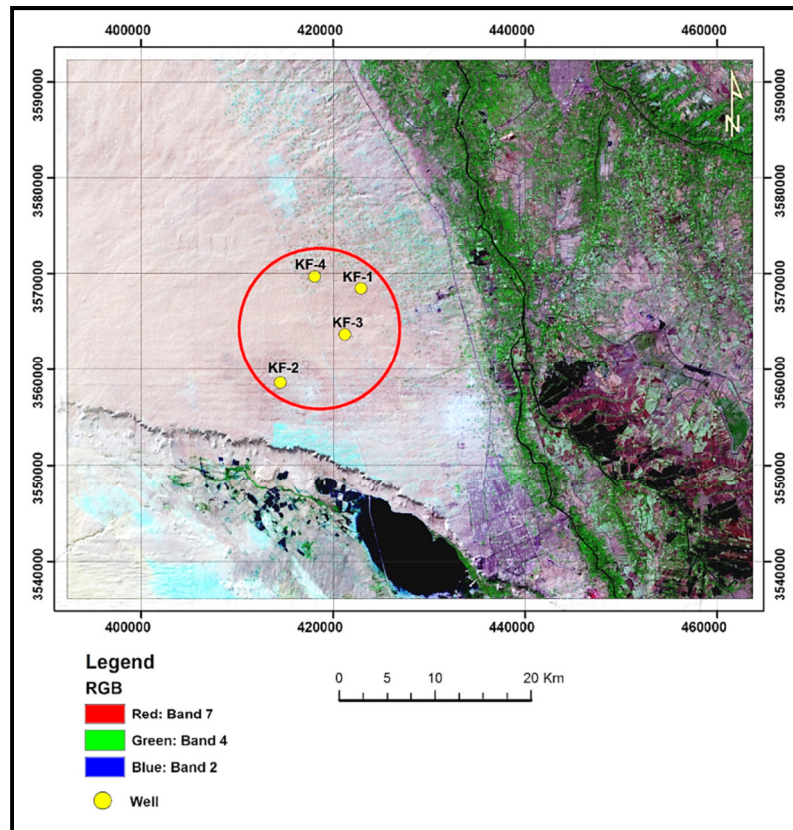

Figure 1. Location map of the study area

Figure 2. Location of wells for Kifl Oil Field in the study area

1.4 Geological Setting

The position of the study area locates within the stable shelf and unstable Shelf. Most of the study area is covered by Quaternary deposits represented by Gypcrete ,Slope deposits ,Flood Plain deposits ,Shallow depression deposits, Sabkha deposits, Marsh deposits,. Aeolian deposits, Valley fill deposits, Anthropogene deposits. Pre-Quaternary rocks are (Eocene-Miocene) represented by Dammam, Euphrates, Fatha, Injana, and Dibdibba Formations, as shown in (Figure 3). The stratigraphic succession is described by (Barwary and Slewa, 1994; Barwary and Slewa, 1995).

2. Methodology

2.1 Data Collection

The present study depends on the following available data:

One scene of Landsat 8 (OLI) is acquisitions in 1-8-2015 (Path 168/ Row 38) in a spatial resolution of 30m for 8 bands, 15m for panchromatic band, and 100m for 2 thermal bands, which downloaded from the Website of USGS as illustrated in (Table 1) and ancillary data besides the field data.

2.2 Software

The following software packages have been used.

1-Erdas Imagine V.13 software was used to produce highly accurate multispectral images, create many kinds of images with various uses such as classification, geometric correction, noise removal , enhancement (spatial and spectral).

2-ArcGIS V.10.2 software was used to management and analyses of data. Digitize geological map and topographical features, drawing maps, maps analysis, display the digital data of maps.
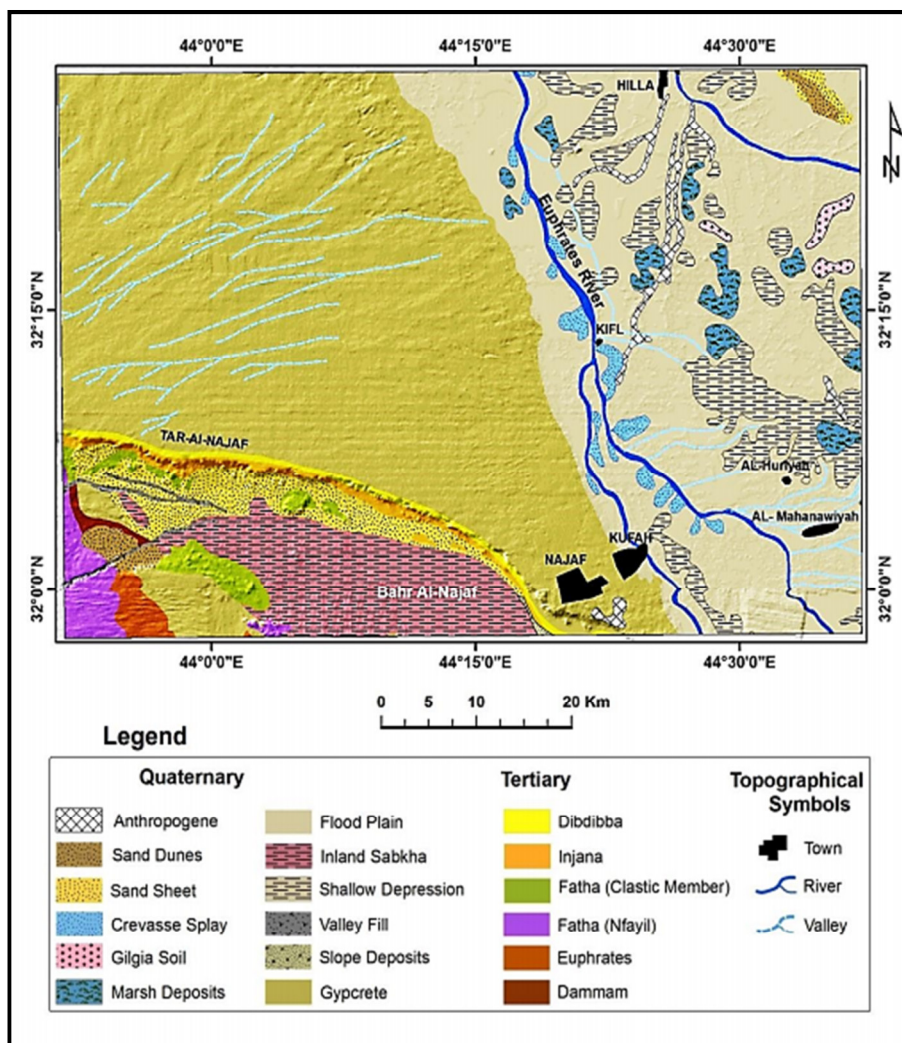
Figure 3. Geological map of the study area

Table 1. Spectral and Spatial Characteristics of Landsat 8 (OLI) (USGS, 2016)

Landsat 8 Operational Land Imager (OLI) and Thermal Infrared Sensor (TIRS) Launched February 11, 2013	Bands	Wavelength (micrometers)	Resolution (meters)
	Band 1 - Coastal aerosol	0.43 - 0.45	30
	Band 2 - Blue	0.45 - 0.51	30
	Band 3 - Green	0.53 - 0.59	30
	Band 4 - Red	0.64 - 0.67	30
	Band 5 - Near Infrared (NIR)	0.85 - 0.88	30
	Band 6 - SWIR 1	1.57 - 1.65	30
	Band 7 - SWIR 2	2.11 - 2.29	30
	Band 8 - Panchromatic	0.50 - 0.68	15
	Band 9 - Cirrus	1.36 - 1.38	30
	Band 10 - Thermal Infrared (TIRS) 1	10.60 - 11.19	100 * (30)
	Band 11 - Thermal Infrared (TIRS) 2	11.50 - 12.51	100 * (30)

2.3 Pre-processing
In this research the Images were imported into ERDAS software from the GEOTIFF format and stack layers (bands) with converted to IMG format. The scenes are clipped for the area of interest (AOI) and geo-registered to the same coordinate system (UTM Zone 38N).

2.4 Normalized Difference Vegetation Index (NDVI)
The typical vegetation index is Normalized Difference Vegetation Index (NDVI). It's a calculation used to

identify vegetation and its health through the Levels of chlorophyll detected in the leaves. NDVI is calculated from the visible and near-infrared light reflected by vegetation. (Figure 4).
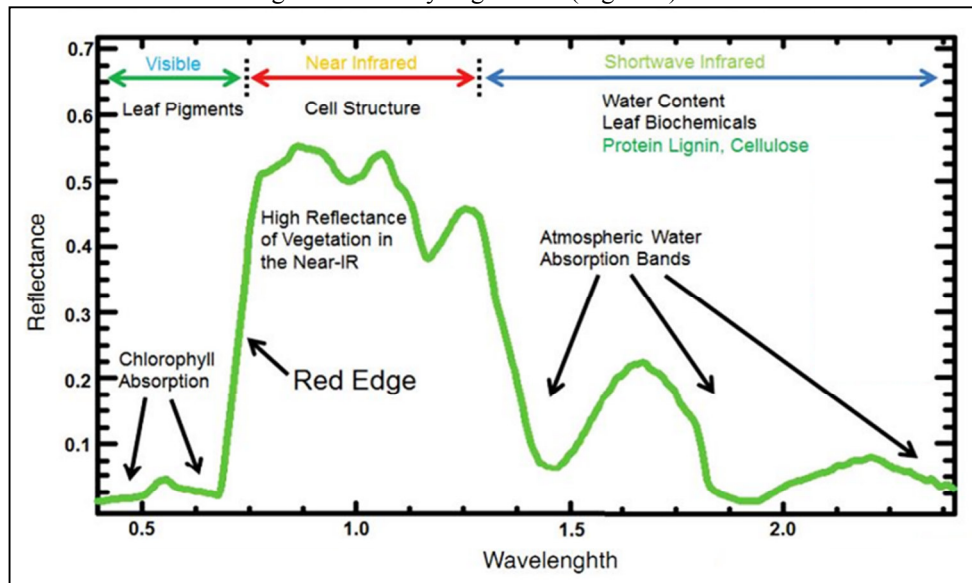

Figure 4. Spectral response curve of vegetation (Imaging Spectroscopy, 2016)

Healthy vegetation absorbs most of the incoming visible light, and reflects a large portion (about 25%) of the near infra-red (NIR) light, but a low portion in the red band (RED). Unhealthy or sparse vegetation reflects more visible light and less NIR light. To apply the NDVI, the following formula is used:

NDVI = (NIR – RED) / (NIR + RED)

(Tucker, 1979; Sabins, 1987; Jensen, 1996).

The NDVI is a common and widely used transformation for the enhancement of vegetation information (Nogi *et al*., 1993, Riano *et al*., 2002). It is used to measure vegetation cover characteristics and incorporated into many forest assessment studies (Wulder, 1998; Roy and Joshi, 2002; Levent and Scot, 2003). It can be used for accurate description of land cover and vegetation classification (Tarpley *et al,*. 1984; Justice *et al.*, 1985). In some cases, multi resolution imagery and integrated analysis method were included along with NDVI for land cover classification (Laporte *et al,*. 1998, Moody, 1998).

The information is usually presented in pseudo color. These techniques are applied with raster and vector geoprocessing using Geographic Information Systems (GIS), to provide very powerful analysis.

Thresholding is carried out in this method. A critical step is the selection of appropriate threshold boundaries between the values of pixels for Normalized Difference Vegetation Index (NDVI)

The quantification of NDVI is relative and not absolute; therefore, it provides a measure of which areas of vegetation are more vigorous than others (Harrison & Garg, 1991).

The result of algorithm is a single band data with NDVI and values ranging from -1 to 1 (Sabins 1996; Jensen 2000). NDVI can highlight enhance specific spectral differences, which cannot be observed in the display of the original color bands (Gutman, 1991) (Figure 5). (Figure 6) shows Histogram of NDVI and (Figure 7) shows NDVI image which is translated into four LULC classes represented by high vegetation density, moderate vegetation density, low vegetation density, and no vegetation classes.

The magnitude of green vegetation was quantified to levels and separated from other classes. The NDVI is directly related to the photosynthetically active radiation within a pixel. The vegetation classification is based on threshold values to classify the NDVI as shown in in (Table 2).

(Table 3) show statistics of NDVI and (Table 4) show vegetation covers of NDVI. (Figure 8) reveal diagram showing the area in Km^2 and percentage of each class of NDVI.
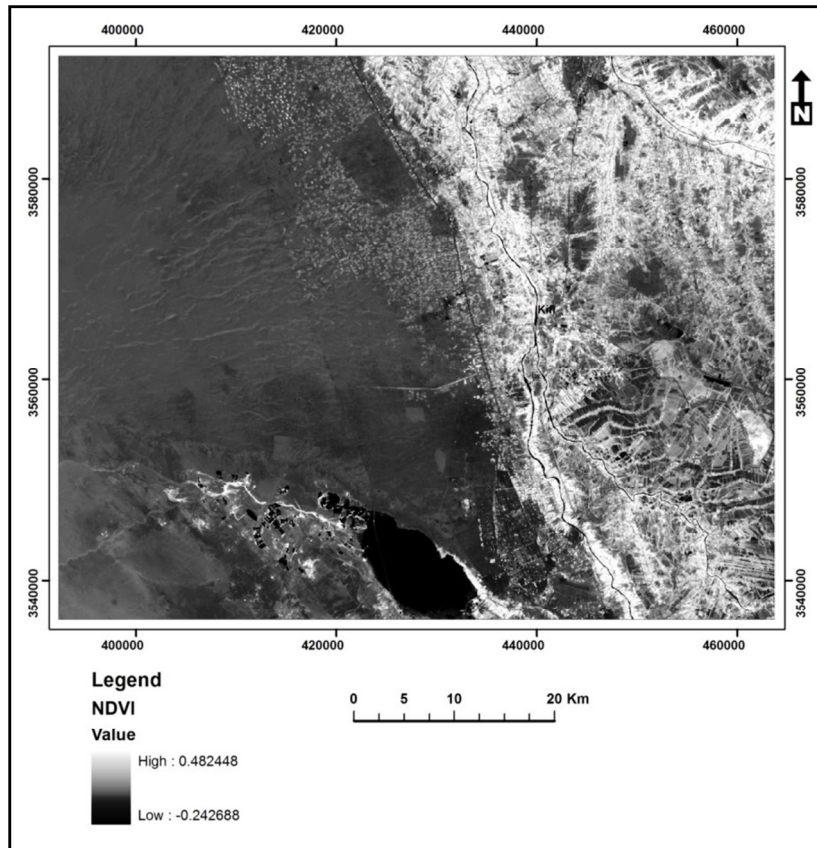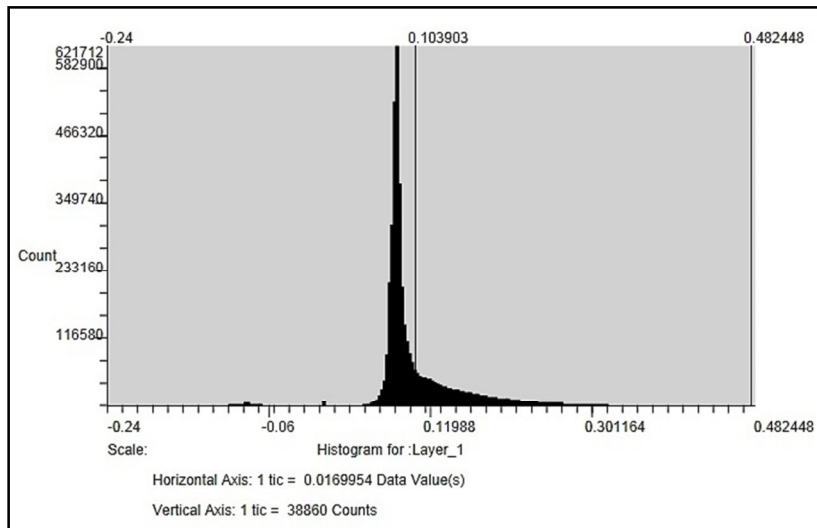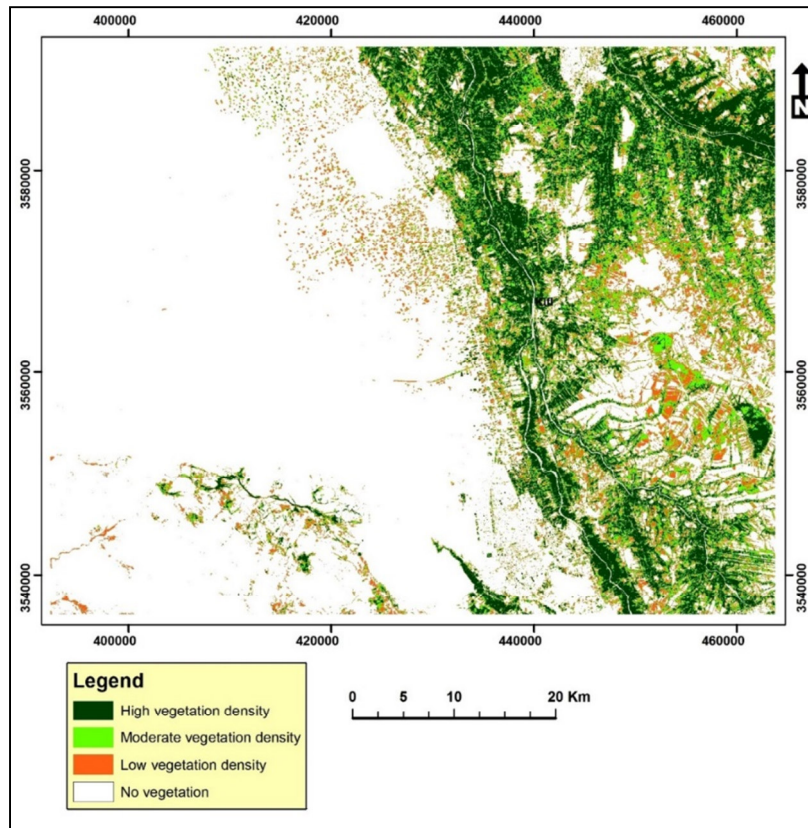
Figure 5. NDVI image

Figure 6. Histogram of NDVI

Figure 7. NDVI image translated into four LULC classes

Table 2. NDVI Thresholding

(NDVI)	Thresholding
High vegetation density	0.4796-0.1595
Moderate vegetation density	0.1567-0.1255
Low vegetation density	0.1227-0.1057
No vegetation	< 0.1057

Table 3. Statistics of NDVI

	Value	Histogram	Total area of NDVI (km²)
Total	38.9246	1307408	
Mean	0.292666	9830	
Minimum	0.105717	0	1177
Maximum	0.479615	53428	
Std.dev.	0.109161	13335	

Table 4. Vegetation covers of NDVI areas

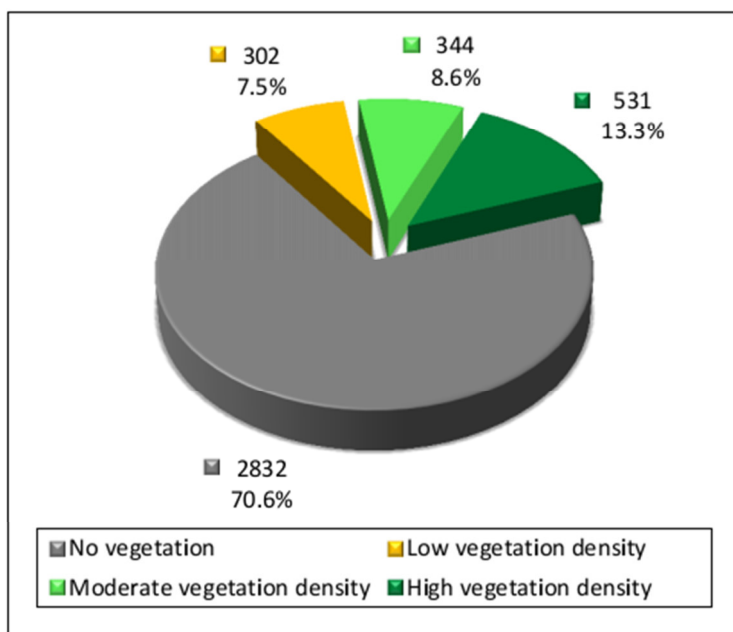| (NDVI)	Surface Area	
	km²	p.%
High vegetation density	531	13.3
Moderate vegetation density	344	8.6
Low vegetation density	302	7.5
No vegetation	2832	70.6

22

Figure 8. Diagram showing area in Km^2 and percentage of each class of NDVI

2.4.1. Extract Hydrocarbon Evidence from NDVI

The two gases that are found in microseepages and also make up the bulk composition, CH4 (methane) and CO2 (carbon dioxide), have absorption features in the generally used reflective (0.4 - 2.5 μm) part of the spectrum (Pieters & Englert,1993). Remote sensing can detect indirect evidence of hydrocarbon seepage, such as botanical and mineralogical alterations that develop due to the presence of hydrocarbons in the soil. Long-term leakage can lead to formation of anomalous oxidation-reduction zones (Schumacher, 1996; Hoeks, 1983). Aerobic and anaerobic bacteria that oxidise the migrating hydrocarbons are, directly or indirectly, responsible for the varied and often complex surface manifestations. Bacterial oxidation of CH4 and the presence of CO2 depletes oxygen from the soil (Smith et al., 2004). Eventually, the soil can even become anaerobic, causing roots of plants to die off (Hoeks, 1983).

Its notes in map of (Figure 7), particularly in right side some of areas are unoccupied by vegetation and other areas have low vegetation density, these areas may give possibility of existence evidence of hydrocarbon as a result of above mention reasons.

To extract hydrocarbon evidence accurately, supervised classification apply on the gray scale image of NDVI by chosen training areas of dark tones pixels that show values of hydrocarbon absorption between (0.0519 to 0.0660) which are very close to minimum value of water absorption in the study area (0.0207). The total number of pixels that have hydrocarbon prospective is 8562 pixels which form area 7.598 km² .The number of pixels that have high hydrocarbon prospective is 687 pixels, which form area 0.781 km² (Figure 9). (Figure 10) show statistics of hydrocarbon seepage and (Figure 11) represent map of hydrocarbon seepage density, in this figure the main paved road between Karbala and Al-Najaf governorates seem low density, this attribute to its width which is less than 30 m, also the density is calculated depend on the area. On the other hand all Kifl Oil Wells locate within the hydrocarbon seepage regions. Also the density of hydrocarbon seepage appear to be distributed along parallel and intersecting lines, these lines could be lineaments or faults which may give acceptable evidence of existence hydrocarbon in the study area.
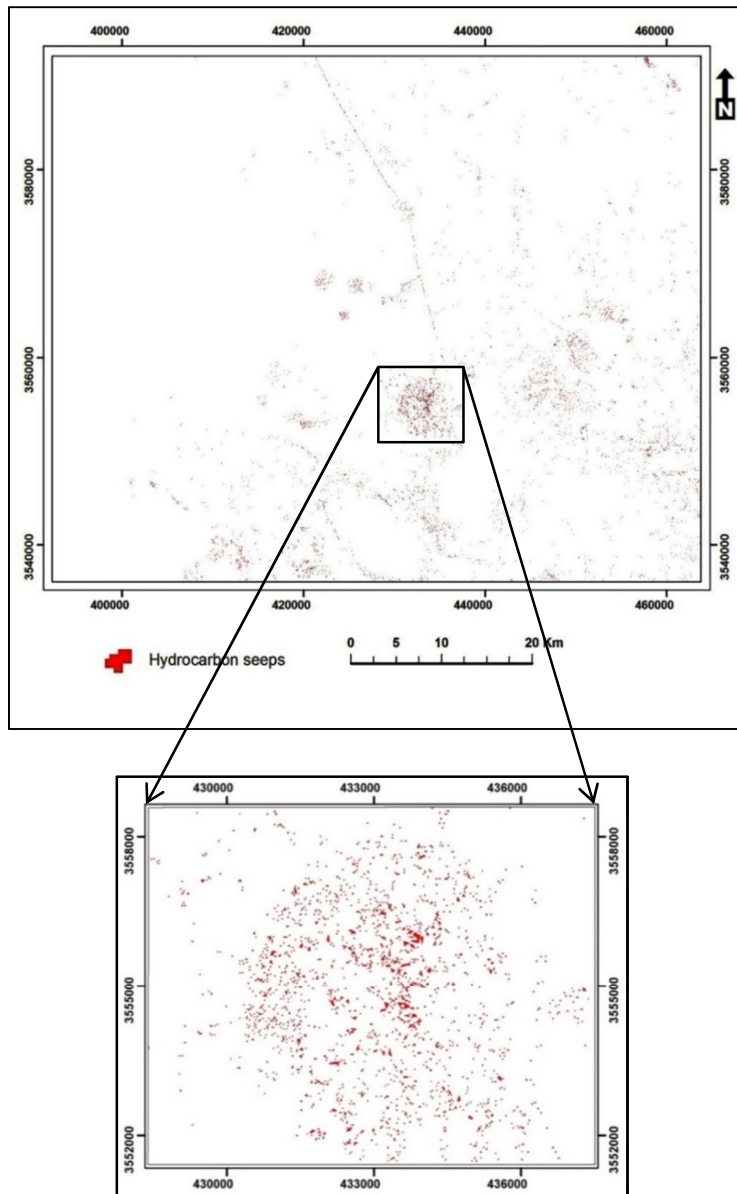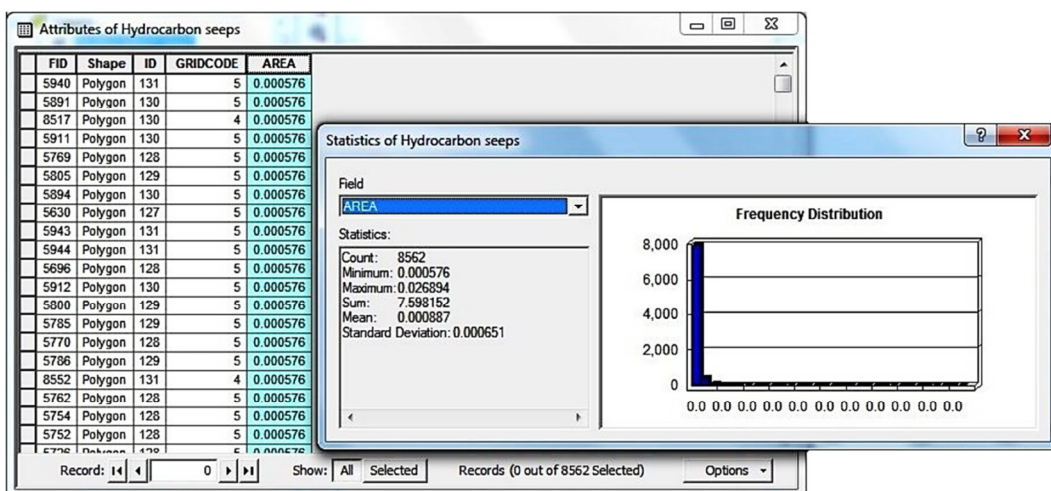
Figure 9. Hydrocarbon seepage map

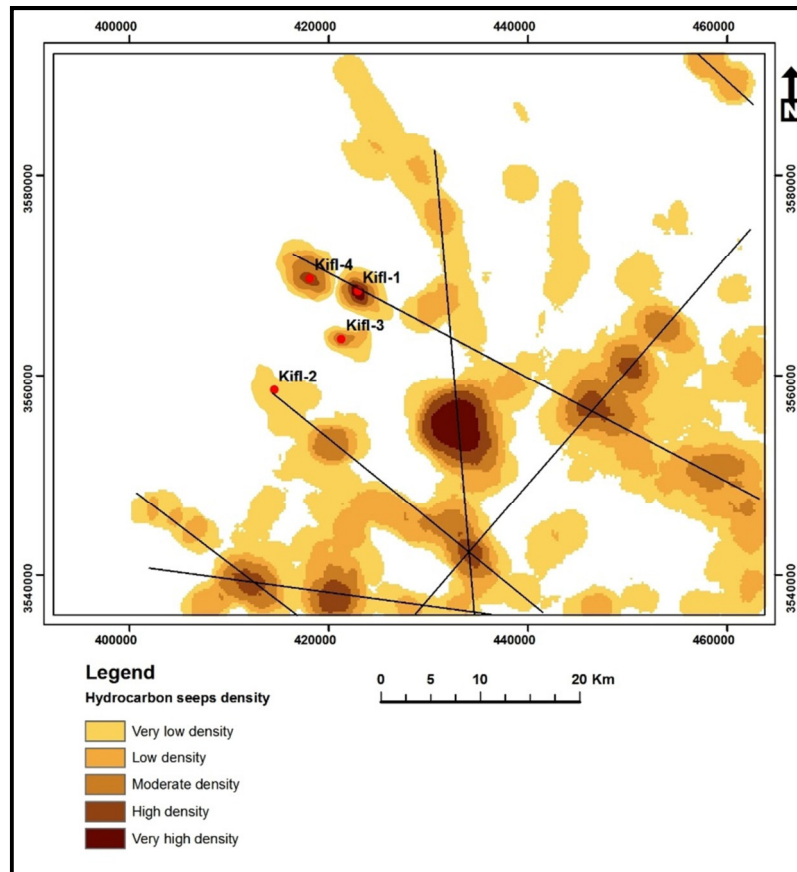Figure 10. Statistics of hydrocarbon seepage

Figure 11. Hydrocarbon seepage density map

For reliability of the results, it had collected samples of spectral signature for three main classes in the study area include hydrocarbon seepage, vegetation, and water; to compare it with other three samples represent the same classes collected from another near area (Scene: Path 169/ Row 37, acquisition in 7-7-2015). The sample of spectral signature of hydrocarbon seepage collected from the main paved road between Karbala and Al-Najaf governorates which this road consist of asphalt (bitumen) in its main component and compare it with sample of spectral signature collected from the Abu Jir seepage zone which is dominated by large bitumen seepages forming crater lakes more than 2 km wide (Jassim & Goff, 2006). More than sample had been collected and compared, (Figure 12. A and B). From this comparison it is found identical behave of the spectral signatures for all three classes whereof gives reliability for the results, the little differences in values of spectral signature of these classes attribute to difference in acquisition date of both scenes which mean difference in factors that effect on pixel values (DN_S) such as atmospheric effects.
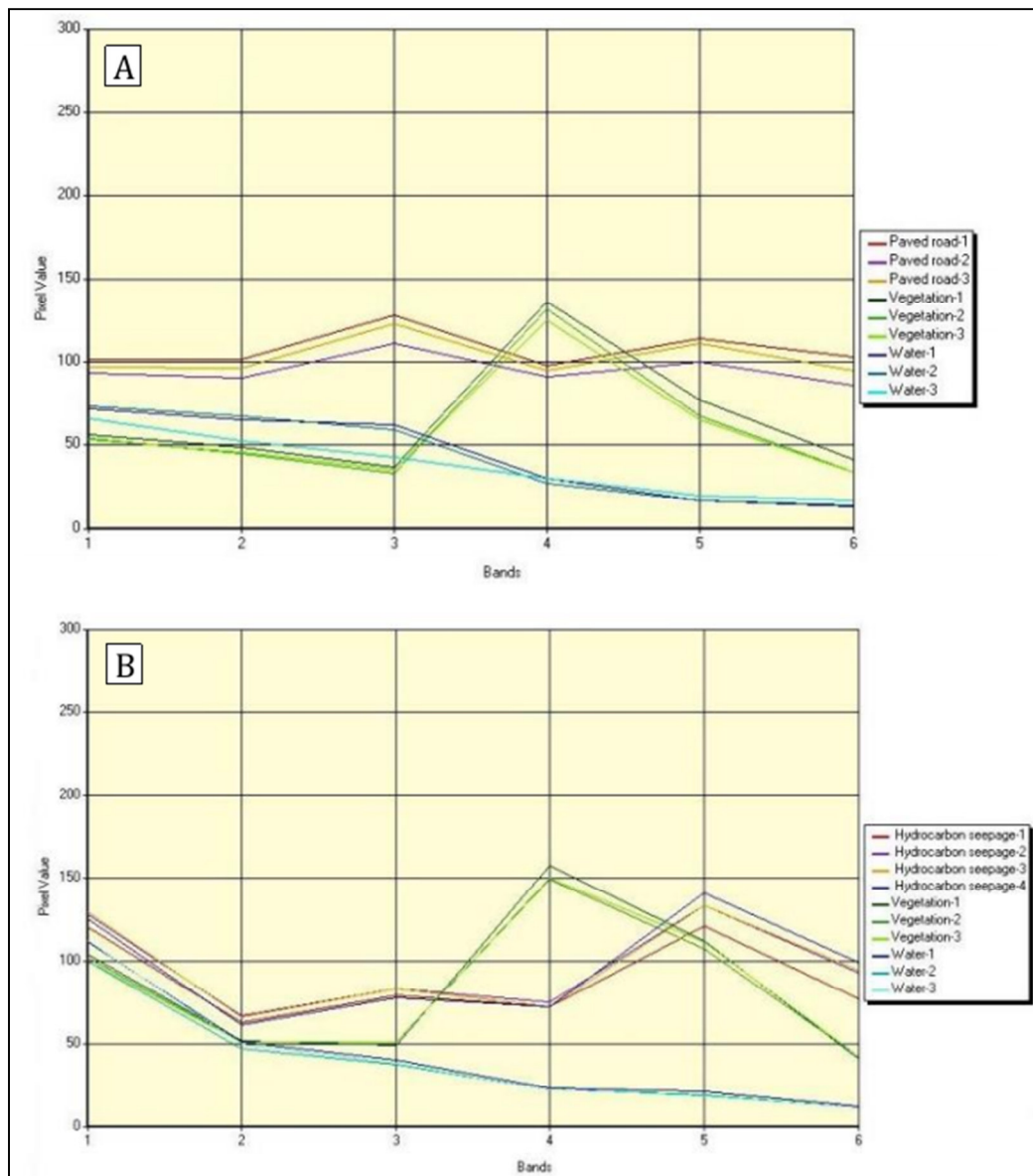
Figure 12. Spectral signature of three classes. (A) In the study area (B) In another near area

3. Conclusions

The vegetation classification is based on threshold values which used to classify the NDVI into four categories: High vegetation density, Moderate vegetation density, Low vegetation density, and no vegetation. In (Figure 7), particularly in right side some of areas are unoccupied by vegetation and other areas have low vegetation density, these areas may give possibility of existence evidence of hydrocarbon as a result of anaerobic soil which is causing roots of plants to die off and finally lead to decrease of vegetation density or absence of vegetation. Accurately hydrocarbon evidence had been done through supervised classification apply on the gray scale image of NDVI by chosen training areas of dark tones pixels that show values of hydrocarbon absorption between (0.0519 to 0.0660), this range of values represent hydrocarbon seepage evidence in the study area which illustrated on the hydrocarbon seepage map and hydrocarbon seepage density map, it can see that all Kifl Oil Wells which are some of them producer of hydrocarbon and other wells have hydrocarbon evidences locate within the hydrocarbon seepage regions. As well as the density of hydrocarbon seepage is distributed along parallel and intersecting lineaments or faults which may give adequate evidence of existence hydrocarbon. Three main classes in the study area include hydrocarbon seepage, vegetation, and water; compared with other three classes collected from another near area, this comparison had been proved that there is identical behave of the spectral signatures for all three classes in both areas. According to the above result the NDVI is effective to identify hydrocarbon seepage in the study area particularly in the regions characterized by vegetation cover.

References

Barwary, A.M. and Slewa, N.A., 1994. The geological map Al-Najaf Quadrangle, sheet NH-38-2, GEOSURV, Baghdad, Iraq.

Barwary, A.M. and Slewa, N.A., 1995. The geological map of Karbala Quadrangle, sheet Ni-38-14, GEOSURV, Baghdad, Iraq.

Gutman, G., 1991. Vegetation indices from AVHRR: An update and future prospects. Remote Sensing and Environment. 35: 121-136.

Harrison, A.R. and Garg P., 1991. Multispectral classification for vegetation monitoring in semi arid landscape susceptible to soil erosion and desertification. Gorden and Breach Science Publishers. Amsterdam

Hoeks, J., 1983. Gastransport in de bodem, Technical report, Instituut voor cultuurtechniek en waterhuishouding, Wageningen, The Netherlands.

Imaging Spectroscopy, 2016. http://www.markelowitz.com/ Hyperspectral.html.

Jassim, S. Z., and Goff, J. C., 2006. Geology of Iraq, First edition Published by Dolin, Hlavin 2732, Prague and Moravian Museum Zelny trh 6, Brno, Czech Republic ISBN 80-7028-287-8.

Jensen, J. R., 1996. Introductory digital image processing: A remote sensing perspective. Second edition, New Jersey, U.S.A: Prentice Hall, 257-278.

Jensen, J.R., 2000. Remote sensing of environment: an earth resource prospective. Prentice Hall, upper saddle River.N.J, UAS.

Justice, C.O., Townshend, J.R.G., Holben, B.N., and Tucker, C.J., 1985. Analysis of the phenology of global vegetation using meteorological satellite data. International Journal of Remote Sensing 6, 1271-1318.

Laporte, N. T., Goetz, S. J., Justice, C. O. and Heinecke, M., 1998. A new land cover map of central Africa derived from multi-resolution, multi-temporal AVHRR data. International Journal of Remote Sensing, 19: 3537–3550.

Levent, G. and Scot, S., 2003. Forest covers change assessment for north central Florida using Landsat Thematic Mapper data. http://www.findarticles.com/p/articles/mi_qa4039/is_200309/ai_n9259261

Moody, A., 1998. Using landscape spatial relationships to improve estimates of landcover area from coarse resolution remote sensing. Remote Sensing of Environment, 64: 202–220.

Nogi, A., Sun, W. and Takagi, M., 1993. An alternative correction of atmospheric effects for NDVI estimation. International Geosciences and Remote Sensing, 3: 1137- 1139.

Pieters, C. and Englert, P., 1993. Remote geochemical analysis: Elemental and mineralogical composition, Cambridge Univ. Press, New York. 593 pp.

Riano, D., Chuvieco, E., Ustin, S., Zomer, R., Dennison, P., Roberts, D. and J. Salas., 2002. Assessment of vegetation regeneration after fire through multitemporal analysis of AVIRIS images in Santa Monica Mountains. Remote Sensing of Environment, 79: 60-71.

Roy, P. S. and Joshi, P. K., 2002. Forest cover assessment in north-east India-the potential of temporal wide swath satellite sensor data (IRS-1C WiFS). International Journal of Remote Sensing, 23 (22): 4881 – 4896.

Sabins, F. F., 1987. Remote Sensing Principles and Interpretation. 2d Ed. H. Freeman and Company, New York.

Sabins, F. F., 1996. Remote Sensing. Principles and Interpretation, 3rd Ed.: W. H. Freeman and Company, New York, 494 pages.

Schumacher, D., 1996. Hydrocarbon-induced alteration of soils and sediments, in Schumacher, D., and Abrams, M.A., eds., Hydrocarbon migration and its near-surface expression: American Association of Petroleum Geologists Memoir 66, p. 71–89.

Schumacher, D., 2001. Petroleum exploration in environmentally sensitive areas: Opportunities for non-invasive geochemical and remote sensing methods, pp. 012-1 – 012-5. Annual Convention of the ASPG.

Smith, K., Steven, M. and Colls, J. 2004. Use of hyperspectral derivative ratios in the red-edge region to identify plant stress responses to gas leaks, remote sensing of environment 92: 207–217.

Tarpley, J. D., Schnieder, S. R. and Money, R. L., 1984. Global vegetation indices from NOAA-7 meteorological satellite. Journal of Climate and Applied Meteorology, 23: 4491-4503.

Tucker, C. J., 1979. Red and Photographic Infrared Linear Combinations for Monitoring Vegetation. Remote Sensing of Environment 8:127-150. http://landsat.usgs.gov/Landsat8_Using_Product.php

United States Geological Survey (USGS), 2016. Landsat, the band designations for the Landsat satellites. http://landsat.usgs.gov/band_designations_landsat_satellites.php

Wulder, M., 1998. Optical remote-sensing techniques for the assessment of forest inventory and biophysical parameters. Progress in physical Geography. 22 (4): 449- 476.